1000-0569/2012/028(07)-2145-57 *Acta Petrologica Sinica* 岩石学报

西天山特克斯北中酸性火成岩地球化学特征及成因意义*

朱志敏[1,2] 赵振华[1] 熊小林[3]**

ZHU ZhiMin[1,2], ZHAO ZhenHua[1] and XIONG XiaoLin[3]**

1. 中国科学院广州地球化学研究所,矿物学与成矿学重点实验室,广州 510640
2. 中国科学院研究生院,北京 100049
3. 中国科学院广州地球化学研究所,同位素地球化学国家重点实验室,广州 510640

1. *Key Laboratory of Mineralogy and Metallogeny, Guangzhou Institute of Geochemistry, Chinese Academy of Sciences, Guangzhou* 510640, *China*
2. *Graduate University of Chinese Academy of Sciences, Beijing* 100049, *China*
3. *State Key Laboratory of Isotope Geochemistry, Guangzhou Institute of Geochemistry, Chinese Academy of Sciences, Guangzhou* 510640, *China*

2011-11-09 收稿, 2012-03-15 改回.

Zhu ZM, Zhao ZH and Xiong XL. 2012. Geochemistry and geodynamics of intermediate-acid igneous rocks in northern Tekesi, Western Tianshan Mountains. *Acta Petrologica Sinica*, 28(7): 2145 – 2157

Abstract A large number of intermediate-acidic igneous rocks are exposed along Yi-Te Road and in Kulesayi area, the north of Tekesi County, Western Tianshan Mountains, Xinjiang, China. These rocks are quartz-albite porphyry along Yi-Te Road and quartz diorite and granodiorite in Kulesayi area. They were produced during subducting of the Paleo-Asian oceanic crust. According to their geochemical features and isotopic compositions, the quartz-albite porphyries are typical island/continental arc rocks, and quartz diorite and granodiorite have the compositions of adakite characteristics and may have been produced by slab melting. The earlier cold subducted slab dehydrated before it could begin to melt, and the released fluid ascented into the mantle wedge, which caused melting of mantle wedge and succedent crust-mantle interaction, giving rise to the typical arc magmatism in Yi-Te Road area. As the subduction of oceanic crust continued, the newly formed plate close to the ridge would be hot enough to melt in a shallower depth leaving garnet and rutile as residual phases. This process gave rise to adakitic magmatism in Kulesayi area. Secondary ion microprobe (SIMS) zircon U-Pb dating indicates the Kulesayi porphyry crystallized at the age of 342.5 ± 2.3Ma, which means the Paleo-Asian Ocean (South Tianshan Ocean) had not been completely closed in the Early Carboniferous. These results show that the massive magmatism along southern margin of Yili-Central Tianshan plate was triggered by continuing subduction of South Tianshan Oceanic crust. As thus in Carboniferous, crust growth in Western Tianshan Mountains was possibly mainly horizontal accretion, and the accretion materials may contain oceanic slab (adakite) and mantle wedge components.

Key words Western Tianshan Mountains; Arc volcanic rocks; Adakite; Zircon U-Pb dating; Crust growth

摘 要 新疆西天山特克斯县城北部伊特公路沿线和库勒萨依出露大量中酸性火成岩,伊特公路沿线为石英钠长斑岩,库勒萨依为石英闪长斑岩和花岗闪长斑岩。岩石地球化学和同位素组成研究表明,前者为典型的岛(陆)弧带火成岩,而后者具有埃达克岩的成分特征,两者均为古亚洲洋壳在俯冲过程中岩浆活动的产物。早先俯冲的较冷洋壳板片在深处脱水诱发上覆地幔楔熔融,熔体上升并经历壳幔相互作用等过程引发伊特公路一带弧岩浆活动;由于洋壳持续俯冲,后来新形成的靠近洋脊的年轻板片由于高热在较浅处直接发生部分熔融形成埃达克岩浆,并上侵至库勒萨依一带。库勒萨依斑岩体 SIMS 锆石 U-Pb 年龄为 342.5 ± 2.3Ma,属于早石炭世。两组中酸性火成岩的地球化学特征表明,古亚洲洋(南天山洋)在早石炭世还未完全闭合,洋壳向北的持续俯冲过程造成伊犁-中天山板块南缘广泛的岩浆活动,此时西天山陆壳增生方式主要为侧向增生,增生物质主要为洋壳板片(埃达克岩)和洋壳板片流体交代的地幔楔成分。

关键词 岛弧火成岩;埃达克岩;锆石 U-Pb 年龄;地壳增生;西天山

中图法分类号 P588.13;P597.3

---

* 本文受国家重点基础研究发展计划(973)项目(2007CB411303)和国家自然科学杰出青年基金项目(40825010)联合资助.

第一作者简介:朱志敏,男,1984 年生,博士生,矿物学、岩石学、矿床学专业,E-mail: zhu_zhimin@126.com

** 通讯作者:熊小林,男,研究员,博导,岩石学专业,E-mail: xiongxl@gig.ac.cn

© 1994-2012 China Academic Journal Electronic Publishing House. All rights reserved. http://www.cnki.net

1 引言

俯冲带出露的玄武岩-安山岩-英安岩-流纹岩绝大多数是由受俯冲板片流体交代过的地幔楔熔融以及熔体发生壳幔相互作用等过程形成的(Gill,1981; Martin,1999),它们富集大离子亲石元素和亏损 Nb、Ta、Ti 等高场强元素。研究发现,热的洋壳在俯冲过程中可能直接部分熔融而产生埃达克岩浆,相比普通弧系列岩浆,埃达克岩还具有高 Sr、Al 含量和亏损重稀土等特征(Defant and Drummond,1990)。对这些火成岩的研究能够揭示俯冲-造山过程、壳幔作用以及大陆形成和演化等信息(Martin,1999)。

西天山造山带位于中亚造山带南缘,是古亚洲洋演化史上的一个重要构造域(高俊等,2009)。一般认为古生代以来,塔里木和西伯利亚板块之间的古亚洲洋消减闭合,塔里木、准噶尔、哈萨克斯坦等板块的俯冲-碰撞-增生形成天山(Gao *et al.*,1998,2009; Jahn,2004; Xiao *et al.*,2004,2009; 李锦轶等,2006; Windley *et al.*,2007)。在此过程中,西天山地区发育了大量石炭纪火成岩(如朱永峰等,2005,2006a,2010; 龙灵利等,2008; Zhu *et al.*,2009; Han *et al.*,2010等),其中不乏埃达克岩(如王强等,2003,2006; 熊小林等,2005; 赵振华等,2006; Wang *et al.*,2007; 李永军等,2008a; Tang *et al.*,2010; 朱明田等,2011等)。然而,对于这些石炭纪火成岩形成的构造环境尚存在争议:一些学者认为这些火成岩形成于岛(陆)弧环境(朱永峰等,2005; 李锦轶等,2006; 龙灵利等,2008; Xiao *et al.*,2009,2010; Wang *et al.*,2009; 朱志新等,2011);部分学者认为这些火成岩与裂谷活动(车自成等,1996; Xia *et al.*,2004)或地幔柱活动有关(夏林圻等,2008);还有学者认为西天山早石炭世火成岩形成于岛弧环境,而中-晚石炭世的火成岩可能与后碰撞环境岩浆活动有关(Gao *et al.*,2009; Han *et al.*,2010);也有学者认为本区在早石炭世-晚二叠世属于后碰撞环境(王京彬和徐新,2006)。本文通过对西天山特克斯北的两个火成岩体研究发现,伊特公路沿线的石英钠长斑岩具有典型的弧火成岩浆特征,而库勒萨依出露的石英闪长斑岩和花岗闪长斑岩与埃达克岩地球化学特征一致。本文报道了这些岩石的年代学、岩石地球化学和 Sr、Nd 同位素组成特征,并讨论它们的成因和对西天山古生代地壳增生过程的指示意义。

2 地质背景和岩石学简述

研究区位于特克斯县城以北的乌孙山东段,构造上属于伊犁-中天山板块(图 1a)。伊犁-中天山板块位于西天山中

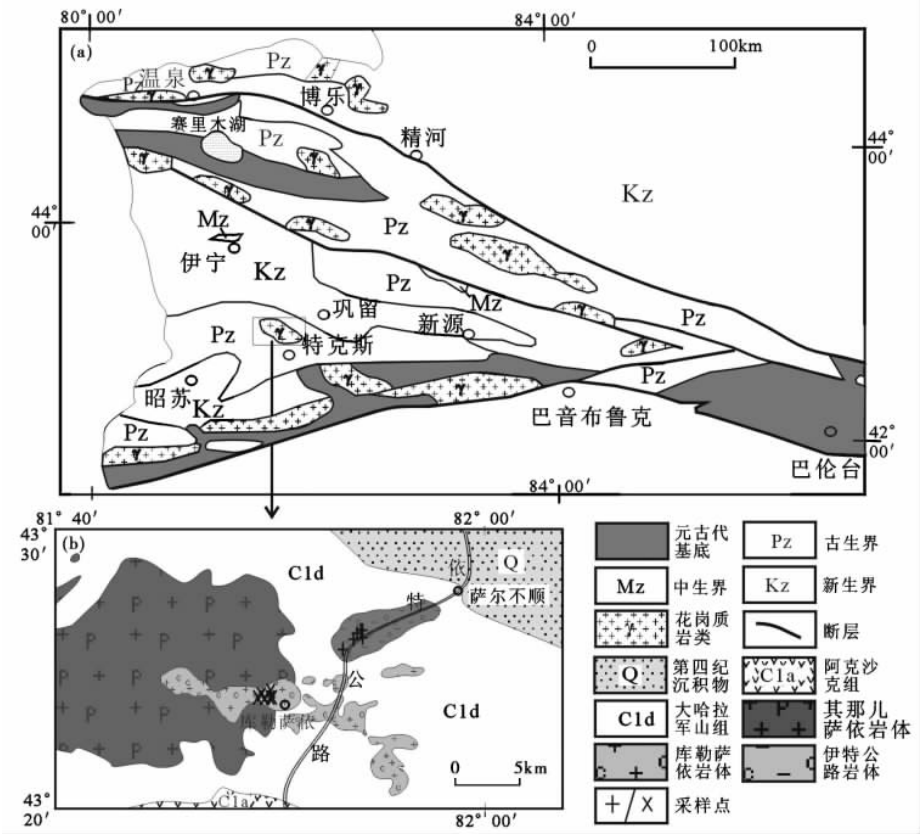


图 1 西天山地质简图(a,据朱志敏等,2010 修改)及特克斯北地质简图(b,据李永军等,2007 修改)中酸性岩采样位置

Fig. 1 Simplified geological map of western Tianshan Mountain (a, after Zhu *et al.*, 2010) and the sketch geological map of intermediate-acid igneous rocks from northern Tekesi area (b, after Li *et al.*, 2007) with sample locations

© 1994-2012 China Academic Journal Electronic Publishing House. All rights reserved. http://www.cnki.net

部,被北部中天山北缘断裂和南部的尼古拉耶夫-那拉提山北坡断裂围成一个向东逐渐尖灭的楔形地体(龙灵利等,2008; Gao *et al*.,2009)。中-晚古生代时,西南天山古亚洲洋(南天山洋)壳的俯冲消减和碰撞造山,引发本区石炭纪大规模的岩浆作用(肖文交等,2006; 高俊等,2009; Zhu *et al*.,2009)。研究区主要分布有早石炭世大哈拉军山组钙碱性岛弧火山岩-次火山岩,包括玄武安山岩、英安岩、流纹岩、钠长斑岩以及同质火山碎屑岩(李注苍等,2006)、早石炭世阿克沙克组浅海相碳酸盐岩和火山碎屑沉积岩、晚石炭世伊什基里克组双峰式裂谷火山岩、晚石炭世东图津河组海相碎屑岩、晚石炭世科古琴山组陆相碎屑岩和一些二叠纪陆相碎屑岩-双峰式火山岩等(朱永峰等,2006a; 李永军等,2007,2010)。局部地层出露晚泥盆特克斯达坂组钙碱性岛弧火山岩(朱永峰等,2006b),特克斯县城东北部出露一定规模的晚石炭世基性-超基性侵入岩,主要为辉长岩和辉绿岩(薛云兴和朱永峰,2009; 朱志敏等,2010)。

样品采集工作集中在特克斯北部的伊特公路沿线和库勒萨依一带(图1b)。伊特公路沿线的岩体位于大哈拉军山组火山岩中,它与大哈拉军山组火山岩属于本区石炭纪地层中同组级岩石地层单位(李永军等,2008a)。伊特公路沿线岩体主要为石英钠长斑岩,呈肉红色到浅灰白色,中细粒斑状结构。斑晶为钠长石和角闪石,基质为钠长石,少量碱性长石、石英和黑云母。库勒萨依岩体位于伊特公路岩体东南约10km处,呈小岩体和岩枝侵入于早石炭世大哈拉军山组火山岩中,或呈捕虏体包裹于早二叠世其那尔萨依岩体中(李永军等,2007)。库勒萨依中酸性岩体主要为石英闪长斑岩和花岗闪长斑岩,部分岩体已有钼矿化报道(李永军等,2008a,2010)。石英闪长斑岩和花岗闪长斑岩均具斑状结构,基质微细粒。前者手标本浅肉色-灰白色,斑晶主要为较自形板状斜长石,基质为中长石、石英、角闪石和少量黑云母; 后者呈暗灰色,部分样品肉红色,斑晶主要为长柱状-板状更-中长石和长柱状角闪石,碱性长石较少,基质由石英、角闪石和少量钾长石组成。

3 同位素年龄

伊特公路沿线岩体石英钠长斑岩(次火山岩)属于大哈拉军山组火山岩系列岩石(李永军等,2008a),前人在区域地质调查中,于本区采样点东北约10km处伊特公路萨尔不顺沟获得大哈拉军山组全岩Rb-Sr等时线年龄为351±2Ma(李永军等,2008b),这与新源南部同套岩体中获得的玄武安山岩-玄武岩SHRIMP锆石U-Pb年龄(352~355Ma,朱永峰等,2005; Zhu *et al*.,2009)一致,年龄可靠性较高,因而351Ma可以代表伊特公路沿线的石英钠长斑岩形成年龄。

库勒萨依岩体的年龄使用锆石U-Pb法测定。本文选用的样品为采自库勒萨依的中粒斑状花岗闪长岩(样品编号为XTT845),样品新鲜、无蚀变,岩石样品经粉碎后用标准技术进行锆石分选。锆石样品靶的制备和U-Pb定年均由中国科学院地质与地球物理研究所离子探针实验室完成,锆石样品靶的制备方法及U-Pb同位素详细的分析流程见Li *et al*.(2009)。锆石阴极发光图像在中国科学院广州地球化学研究所JEOL JXA-8100型电子探针上完成,定年在中国科学院地质与地球物理研究所离子探针实验室的Cameca IMS-1280型二次离子质谱仪(SIMS)上进行。锆石样品的U-Th-Pb同位素比值用标准锆石Temora校正获得(Whitehouse *et al*.,1997),U、Th含量用标准锆石91500校正获得(Wiedenbeck *et al*.,1995),普通Pb用测量的^{204}Pb进行校正。由于测得的普通Pb含量非常低,可以认为普通Pb主要来源于制样过程中带入的表面Pb污染,用现代地壳的平均Pb同位素组成作为普通Pb组成进行校正(Li *et al*.,2009)。单点分析的同位素比值及年龄误差为1σ,U-Pb平均年龄误差为95%置信度,数据结果用IsoPlot软件处理完成(Ludwig,2003)。

从测试样品的锆石阴极发光图像(CL图像)中可以看出,锆石清晰透明,无裂纹,自形程度高,多呈长柱状,颗粒较均匀,粒径较大长宽比多在2∶1~3∶1之间,发育典型的基性岩浆成因的韵律环带结构(图2)。共测定了20颗锆石,U、Pb同位素分析及年龄测定结果见表1。

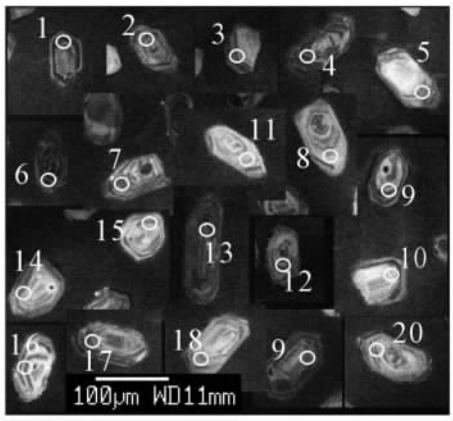


图2 特克斯库勒萨依斑岩(XTT845)的锆石阴极发光(CL)图像

Fig. 2 The cathode luminescence (CL) images of zircons from sample XTT845

在谐和年龄图解中,所有U-Pb年龄数据成群集中分布在谐和曲线上(图3),因此用20个测点的$^{206}Pb/^{238}U$年龄的加权平均值342.5±2.3Ma代表库勒萨依花岗闪长岩(埃达克岩)的形成年龄。

4 元素地球化学特征

主量元素和微量元素分析均在中国科学院广州地球化学研究所同位素地球化学国家重点实验室完成,主量元素由XRF(Rigaku100e型X-荧光光谱仪)测定,微量元素由ICP-

© 1994-2012 China Academic Journal Electronic Publishing House. All rights reserved. http://www.cnki.net

表 1 特克斯库勒萨依斑岩(XTT845)的锆石 U-Pb 分析结果

Table 1 U-Pb isotope analyses of zircons in sample XTT845

测点号	U (×10⁻⁶)	Th (×10⁻⁶)	Th/U	$f_{206}^{\#}$ (%)	$^{207}Pb/^{206}Pb$	±1σ (%)	$^{207}Pb/^{235}U$	±1σ (%)	$^{206}Pb/^{238}U$	±1σ (%)	t207/206 (Ma)	±1σ (%)	t207/235 (Ma)	±1σ (%)	t206/238 (Ma)	±1σ (%)
XTT845@1	1465	1178	0.804	1.01	0.05386	2.57	0.39972	2.99	0.0538	1.53	365.3	56.9	341.4	8.7	338.0	5.1
XTT845@2	482	319	0.663	0.05	0.05427	1.57	0.41044	2.21	0.0548	1.56	382.4	34.8	349.2	6.6	344.2	5.2
XTT845@3	216	123	0.568	0.22	0.05171	2.30	0.39286	2.77	0.0551	1.55	272.6	51.8	336.5	8.0	345.8	5.2
XTT845@4	595	499	0.838	0.02	0.05357	1.12	0.40922	1.90	0.0554	1.54	353.1	25.1	348.3	5.6	347.6	5.2
XTT845@5	200	147	0.732	0.17	0.05307	2.72	0.40081	3.12	0.0548	1.53	332.0	60.5	342.2	9.1	343.7	5.1
XTT845@6	957	825	0.863	0.14	0.05350	1.04	0.39718	1.83	0.0538	1.50	349.9	23.3	339.6	5.3	338.1	4.9
XTT845@7	456	327	0.717	0.25	0.05077	2.17	0.37439	2.65	0.0535	1.51	230.6	49.4	322.9	7.3	335.8	4.9
XTT845@8	246	166	0.673	0.00	0.05534	2.25	0.42509	2.71	0.0557	1.51	426.1	49.4	359.7	8.2	349.5	5.1
XTT845@9	422	328	0.777	0.12	0.05281	1.65	0.39202	2.23	0.0538	1.50	320.7	37.0	335.8	6.4	338.0	4.9
XTT845@10	154	104	0.677	0.48	0.05599	4.15	0.42366	4.46	0.0549	1.62	452.0	89.6	358.7	13.6	344.4	5.4
XTT845@11	247	181	0.731	0.21	0.05270	2.71	0.39798	3.17	0.0548	1.64	315.8	60.5	340.2	9.2	343.8	5.5
XTT845@12	226	158	0.699	0.23	0.05284	2.35	0.39747	2.79	0.0546	1.51	321.9	52.5	339.8	8.1	342.4	5.0
XTT845@13	984	1330	1.351	0.58	0.05302	2.26	0.40620	2.72	0.0556	1.50	329.6	50.6	346.1	8.0	348.6	5.1
XTT845@14	176	129	0.736	0.12	0.05693	2.10	0.43357	2.60	0.0552	1.53	488.8	45.7	365.7	8.0	346.6	5.2
XTT845@15	208	176	0.848	0.18	0.05153	2.43	0.38482	2.86	0.0542	1.51	264.6	54.9	330.6	8.1	340.0	5.0
XTT845@16	420	586	1.395	0.39	0.05353	2.01	0.39662	2.52	0.0537	1.52	351.4	44.7	339.2	7.3	337.4	5.0
XTT845@17	424	288	0.679	0.00	0.05413	1.42	0.41064	2.07	0.0550	1.50	376.6	31.7	349.3	6.1	345.2	5.1
XTT845@18	290	259	0.892	0.09	0.05376	1.81	0.39810	2.37	0.0537	1.52	361.0	40.3	340.3	6.9	337.2	5.0
XTT845@19	222	160	0.720	0.20	0.05102	2.81	0.38766	3.20	0.0551	1.53	241.9	63.6	332.7	9.1	345.8	5.2
XTT845@20	278	184	0.663	0.08	0.05416	1.75	0.40506	2.36	0.0542	1.59	377.6	38.9	345.3	6.9	340.5	5.3

注: $f_{206}^{\#}$ 为普通 ^{206}Pb 占总 ^{206}Pb 的比例

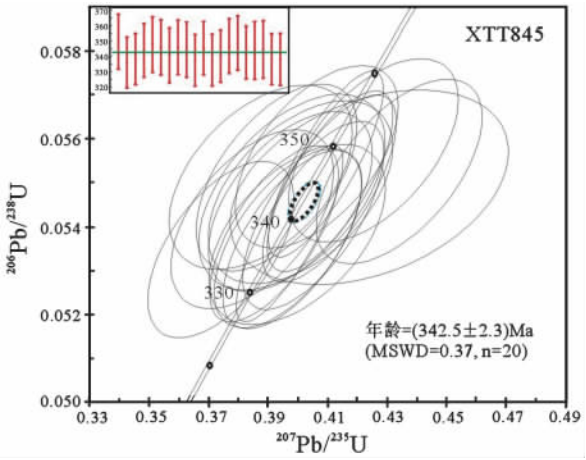


图 3 库勒萨依斑岩体中花岗闪长岩的锆石 U-Pb 一致曲线

Fig. 3 The U-Pb concordia diagram for zircon of Kulesayi porphyry from northern Tekesi

MS(PE Elan 6000 型)测定,前者分析精度优于 5%,后者优于 7%(绝大多数优于 3%),仪器的工作条件和分析方法等见刘颖等(1996)。用于主量元素和微量元素分析的样品经粗碎后再用碳化钨钵体磨成可过 200 目筛的粉末,每次换磨样品时,均先用自来水冲洗钵体并用酒精棉擦拭,以防止样品间相互污染。特克斯北中酸性火成岩的主量元素和微量元素测定结果见表 2。

从表 2 可以看出,伊特公路沿线的岩体和库勒萨依岩体在地球化学特征上明显不同。伊特公路剖面出露的石英钠长斑岩 SiO_2 含量在 62.04% ~ 69.86%,具有较高的 Al_2O_3(14.22% ~ 16.2%)和 K_2O 含量(4.02% ~ 6.48%),富碱($Na_2O + K_2O = 7.94\% \sim 9.51\%$),$Na_2O$ 相对库勒萨依岩体较低,Na_2O/K_2O 值低(0.39 ~ 1.15),在 K_2O-SiO_2 图解中均落入橄榄玄粗岩系列(图 4)。A/CNK 范围为 0.9 ~ 1,属于准铝质(图 5)。库勒萨依岩体具有中酸性火成岩(安山质-英安质)的成分特征: Si_2O 含量为 57.06% ~ 70.74%,具有较高的 Na_2O(3.99% ~ 5.69%)和 Al_2O_3(15.84% ~ 17.00%)含量,Na_2O/K_2O 值高(0.93 ~ 2.29),$Na_2O + K_2O = 6.46\% \sim 8.64\%$,在 K_2O-SiO_2 图中主要落于高钾钙碱性系列,少数样品达到橄榄玄粗岩系列(图 4)。$Mg^{\#}$ 变化范围较大(33.1 ~ 59.7),平均值为 40.9,A/CNK 范围为 0.9 ~ 1.1,属于准铝质到弱过铝质火成岩(图 5)。

在 Na-K-Ca 三角图中(图 6),可以明显看出两组岩石样品分布于不同的岩石类型区域: 伊特公路沿线的样品主要落

© 1994-2012 China Academic Journal Electronic Publishing House. All rights reserved. http://www.cnki.net

表 2 特克斯北中酸性火成岩主量元素(wt%)和微量元素($\times 10^{-6}$)组成

Table 2 Major(wt%) and trace elements($\times 10^{-6}$) composition of intermediate-acid igneous rocks from northern Tekesi area

样品号	XTT838	XTT839	XTT840	XTT841	XTT842	XTT843	XTT845	1*	2*	3*	4*	5*
位置	库勒萨依											
经度 E	81° 50. 304′	81° 50. 285′	81° 50. 157′	81° 50. 157′	81° 50. 157′	81° 49. 925′	81° 49. 795′					
纬度 N	43° 23. 945′	43° 23. 937′	43° 24. 070′	43° 24. 070′	43° 24. 070′	43° 24. 100′	43° 24. 142′					
SiO_2	60. 88	66. 88	68. 49	68. 64	57. 25	67. 22	68. 27	70. 74	67. 37	63. 94	63. 71	63. 69
TiO_2	0. 50	0. 62	0. 46	0. 42	0. 75	0. 54	0. 50	0. 42	0. 51	0. 72	0. 85	0. 58
Al_2O_3	18. 60	14. 98	15. 17	15. 49	16. 27	15. 60	15. 23	15. 01	15. 40	15. 52	15. 60	16. 27
$Fe_2O_3^T$	3. 86	3. 79	3. 30	3. 02	6. 58	3. 67	3. 26	3. 29	4. 89	6. 15	5. 93	5. 56
MnO	0. 07	0. 07	0. 07	0. 07	0. 23	0. 07	0. 07	0. 08	0. 08	0. 10	0. 09	0. 13
MgO	1. 19	1. 31	1. 28	1. 11	4. 92	1. 35	1. 29	0. 91	1. 22	1. 70	1. 70	2. 67
CaO	1. 88	1. 90	2. 39	2. 99	5. 36	3. 23	2. 69	1. 83	1. 31	3. 37	3. 22	2. 55
Na_2O	7. 30	4. 16	3. 65	3. 81	3. 65	3. 80	3. 78	4. 56	4. 32	3. 58	3. 88	4. 49
K_2O	3. 38	4. 34	3. 62	3. 46	2. 76	3. 50	3. 75	3. 26	3. 77	3. 87	3. 76	2. 37
P_2O_5	0. 15	0. 18	0. 15	0. 13	0. 24	0. 17	0. 15	0. 14	0. 15	0. 22	0. 25	0. 12
LOI	2. 00	1. 55	1. 20	0. 64	1. 78	0. 66	0. 78					
Total	99. 80	99. 78	99. 78	99. 79	99. 80	99. 79	99. 78	100. 01	98. 69	98. 73	98. 61	98. 04
Na_2O/K_2O	2. 16	0. 96	1. 01	1. 10	1. 32	1. 09	1. 01	1. 40	1. 15	0. 93	1. 03	1. 89
A/CNK	0. 98	1. 00	1. 06	1. 00	0. 87	0. 98	1. 00	1. 05	1. 13	0. 96	0. 96	1. 12
$Mg^{\#}$	38. 0	40. 7	43. 5	42. 1	59. 7	42. 2	44. 0	35. 4	33. 1	35. 4	36. 2	48. 7
Ba	716	590	586	699	779	647	586	804	188	209	74	229
Rb	89. 7	147	113	99. 6	82. 2	99. 0	117	87. 6	26	16. 5	3. 15	6. 4
Sr	376	423	594	558	650	525	562	643	626	543	454	452
Nb	10. 83	10. 44	7. 44	7. 942	7. 86	8. 29	8. 17	2. 69	2. 21	2. 22	1. 52	3. 57
Ta	0. 99	0. 993	0. 75	0. 832	0. 59	0. 843	0. 84	0. 4	0. 4	0. 4	0. 4	0. 4
Y	11. 65	22. 96	14. 91	16. 5	16. 71	18. 57	16. 49	12. 3	14. 2	13. 3	4. 73	13. 5
Zr	234	231	143	188	122	154	158	146	65. 7	69. 2	43. 1	62. 9
Hf	6. 39	6. 855	4. 03	5. 611	3. 38	4. 434	4. 76	3. 63	1. 79	2. 6	1. 2	2. 03
Pb	1. 96	19. 86	18. 58	15. 24	12. 58	14. 73	14. 82					
Th	13. 32	12. 74	13. 93	9. 387	6. 46	11. 36	12. 03	6. 22	18. 3	22. 2	19. 3	15. 4
U	2. 94	3. 181	2. 43	2. 032	1. 64	2. 254	2. 65					
Sc	5. 54	7. 72	5. 88	5. 283	13. 28	4. 524	6. 58	13. 6	27. 4	44. 8	10. 8	36
Ti	2356	3391	2279	2336	3436	2518	2489					
V	47. 38	62. 17	57. 28	40. 85	152. 0	58. 74	61. 82					
Cr	0. 80	5. 271	0. 80	2. 468	183. 0	1. 494	0. 90	78	65	107	112	24. 4
Mn	556	577	554	531	1781	522	534					
Co	14. 32	19. 52	37. 68	36. 67	24. 51	38. 68	40. 84	13. 6	25. 9	21. 8	36. 8	24. 9
Ni	4. 70	5. 204	6. 15	4. 403	62. 65	7. 421	6. 47	14. 8	111	68. 6	130	12. 8
Cu	3. 18	16. 4	44. 76	17. 49	253. 30	45. 02	31. 92					
Zn	59. 15	68	46. 82	41. 72	95. 73	37. 13	43. 57					
Ga	16. 52	17. 67	18. 50	17. 35	19. 91	18. 44	18. 29	27	17. 6	15. 7	10. 5	15. 1
Ge	1. 09	1. 175	1. 47	1. 223	1. 77	1. 264	1. 43					
La	24. 43	31. 72	31. 34	26. 75	27. 28	27. 08	25. 36	13. 4	10. 6	5. 23	5. 17	8. 71
Ce	46. 57	64. 05	56. 94	53. 1	54. 56	51. 44	51. 30	26. 8	18	10	8. 5	15. 5
Pr	5. 38	7. 328	6. 33	5. 988	6. 26	6. 108	6. 17	3. 4	2. 18	1. 43	0. 52	2. 47
Nd	19. 65	26. 6	22. 57	21. 89	21. 96	22. 54	22. 69	16. 3	9. 9	7. 49	3. 49	11. 9
Sm	3. 31	4. 942	3. 75	3. 868	3. 74	4. 142	4. 01	3. 3	2. 64	1. 55	0. 87	2. 64
Eu	0. 81	1. 016	0. 91	0. 94	1. 38	0. 998	0. 94	0. 92	1. 11	0. 78	0. 59	0. 99
Gd	2. 96	4. 248	3. 25	3. 321	3. 34	3. 585	3. 67	3	3. 06	2. 59	1. 06	2. 93
Tb	0. 39	0. 646	0. 46	0. 5	0. 48	0. 515	0. 53	0. 48	0. 5	0. 45	0. 2	0. 51
Dy	2. 11	3. 707	2. 66	2. 776	2. 77	2. 905	3. 03	2. 94	3. 36	3. 23	1. 11	3. 15
Ho	0. 42	0. 741	0. 54	0. 544	0. 57	0. 576	0. 62	0. 52	0. 58	0. 64	0. 2	0. 6
Er	1. 22	2. 09	1. 50	1. 582	1. 65	1. 581	1. 74	1. 7	1. 81	2. 07	0. 64	1. 69
Tm	0. 19	0. 323	0. 24	0. 246	0. 25	0. 245	0. 26	0. 26	0. 26	0. 32	0. 1	0. 26
Yb	1. 37	2. 219	1. 59	1. 714	1. 71	1. 701	1. 78	1. 45	1. 46	1. 66	0. 7	1. 65
Lu	0. 24	0. 361	0. 26	0. 278	0. 28	0. 28	0. 28	0. 18	0. 2	0. 22	0. 07	0. 2
ΣREE	109. 1	150. 0	132. 3	123. 5	126. 2	123. 7	122. 4	74. 65	55. 66	37. 66	23. 22	53. 2
Sr/Y	32. 3	18. 4	39. 8	33. 8	38. 9	28. 2	34. 1	52. 3	44. 1	40. 8	96	33. 5
La/Yb	17. 8	14. 3	19. 7	15. 6	15. 9	15. 9	14. 3	9. 2	7. 3	3. 2	7. 4	5. 3
δEu	0. 79	0. 68	0. 80	0. 80	1. 19	0. 79	0. 75	0. 89	1. 19	1. 19	1. 88	1. 09

© 1994-2012 China Academic Journal Electronic Publishing House. All rights reserved. http://www.cnki.net

续表 2
Continued Table 2

样品号	6*	7*	8*	9*	XTT820	XTT821	XTT822	XTT823	XTT824	XTT825	XTT826
位置	库勒萨依				伊特公路						
经度 E					81°53.942′	81°53.927′	81°53.944′	81°53.915′	81°53.899′	81°53.899′	81°52.392′
纬度 N					43°25.625′	43°25.306′	43°25.212′	43°25.164′	43°25.135′	43°25.135′	43°22.520′
SiO_2	62.70	62.58	58.48	57.06	69.86	65.28	63.46	62.04	66.67	64.61	62.68
TiO_2	0.93	0.92	0.90	0.93	0.49	0.58	1.03	0.92	0.73	0.94	0.97
Al_2O_3	16.07	16.94	17.02	19.31	14.22	15.55	16.20	16.09	15.50	15.95	16.16
$Fe_2O_3^T$	6.12	6.24	7.45	8.60	1.98	2.32	4.59	4.60	3.38	4.29	4.94
MnO	0.11	0.10	0.12	0.12	0.05	0.11	0.11	0.10	0.06	0.12	0.09
MgO	1.63	2.21	2.73	2.54	0.37	0.47	1.48	1.82	1.25	1.50	1.53
CaO	3.22	1.70	2.28	5.83	1.61	3.08	2.62	1.94	0.96	1.60	3.11
Na_2O	4.06	5.10	5.30	4.24	2.54	4.55	4.72	4.40	5.04	4.71	3.92
K_2O	4.13	4.30	4.03	1.85	6.48	4.75	4.12	5.11	4.78	4.48	4.02
P_2O_5	0.25	0.30	0.38	0.29	0.08	0.12	0.27	0.27	0.15	0.23	0.28
LOI					2.11	3.36	1.17	2.52	1.26	1.35	2.09
Total	98.83	100.00	98.26	100.17	99.79	100.17	99.78	99.80	99.78	99.78	99.80
Na_2O/K_2O	0.98	1.19	1.32	2.29	0.39	0.96	1.15	0.86	1.06	1.05	0.97
A/CNK	0.95	1.05	0.99	0.99	1.01	0.85	0.95	0.99	1.02	1.03	0.98
$Mg^{\#}$	34.5	41.2	42.1	36.9	27.1	28.5	38.9	44.0	42.2	40.9	38.0
Ba	101	88	353	540		937		945	821		707
Rb	9.1	18.6	14.3	68.8		105		164	132		144
Sr	593	441	526	794		322		372	207		576
Nb	1.97	1.51	4.75	3.14		11.13		11.88	13.52		11.16
Ta	0.4	0.4	0.4	0.4		0.98		0.96	1.11		0.96
Y	6.48	6.56	14.9	13.6		20.79		23.76	22.57		22.89
Zr	58.6	72.1	82	126		245		243	279		233
Hf	1.81	1.86	2.06	4.06		7.05		6.61	7.49		6.30
Pb						7.88		20.85	24.90		11.94
Th	20.3	64.7	14.6	11.6		11.55		9.69	11.84		10.78
U						3.66		2.35	2.92		2.79
Sc	9.39	21.4	31.6	14		6.71		11.02	8.42		10.88
Ti						2837		5405	3295		5078
V						38.85		76.63	34.35		85.55
Cr	10.6	218	2.4	160		0.34		0.73	0.41		1.08
Mn						847		776	477		726
Co	20.3	27.8	24.4	1.9		12.78		22.06	18.67		20.82
Ni	69.6	83.8	5.5	82.2		4.40		4.49	1.83		6.06
Cu						11.95		33.27	14.52		40.72
Zn						39.44		94.51	76.70		68.30
Ga	14.6	13.4	12.6	23.4		15.32		19.29	18.05		19.97
Ge						0.71		1.04	1.08		1.36
La	3.99	4.53	14.1	16.6		29.93		30.53	35.57		33.33
Ce	7.38	7.99	23.6	31		61.01		63.80	74.01		70.42
Pr	0.74	0.73	3.04	3.46		7.44		8.06	9.11		8.89
Nd	5.14	4.31	15.2	15.4		27.53		32.72	34.76		34.47
Sm	1.44	1.43	3.38	3		5.07		6.14	6.29		6.23
Eu	0.58	0.68	1.17	0.96		1.19		1.48	1.41		1.48
Gd	1.26	1.29	3.61	3.28		4.49		5.57	5.50		5.29
Tb	0.23	0.23	0.62	0.5		0.66		0.81	0.80		0.76
Dy	1.48	1.53	3.73	3.28		3.89		4.69	4.51		4.34
Ho	0.24	0.19	0.71	0.63		0.80		0.94	0.89		0.85
Er	0.71	0.8	2.1	1.64		2.23		2.55	2.50		2.30
Tm	0.11	0.12	0.32	0.26		0.34		0.38	0.37		0.33
Yb	0.7	0.77	1.88	1.7		2.33		2.44	2.48		2.29
Lu	0.08	0.09	0.23	0.2		0.37		0.39	0.40		0.36
ΣREE	24.08	24.69	73.69	81.91		147.3		160.5	178.6		171.3
Sr/Y	91.5	67.2	35.3	58.4		15.5		15.7	9.2		25.2
La/Yb	5.7	5.9	7.5	9.8		12.8		12.5	14.4		14.5
δEu	1.32	1.53	1.02	0.94		0.77		0.77	0.73		0.79

注：* 数据引自李永军等(2008a)；$Mg^{\#} = MgO/(MgO + FeO^T)$ 分子比，FeO^T 表示全铁；$\delta Eu = Eu_N/(Sm_N * Gd_N)^{1/2}$；$Eu_N$，$Sm_N$，$Gd_N$ 为球粒陨石标准化值，球粒陨石数据引自 Boynton (1984)

© 1994-2012 China Academic Journal Electronic Publishing House. All rights reserved. http://www.cnki.net

入正常岛弧 ADR(安山岩-英安岩-流纹岩)区域,而库勒萨依的样品主要落入埃达克岩和太古宙 TTD(奥长花岗岩-英云闪长岩-英安岩)区域。

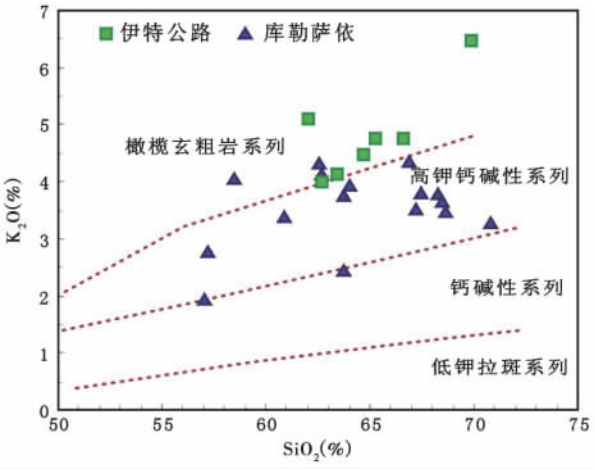


图 4 特克斯北中酸性火成岩 K_2O-SiO_2 图解

Fig. 4 The K_2O-SiO_2 diagram of intermediate-acid igneous rocks from northern Tekesi area

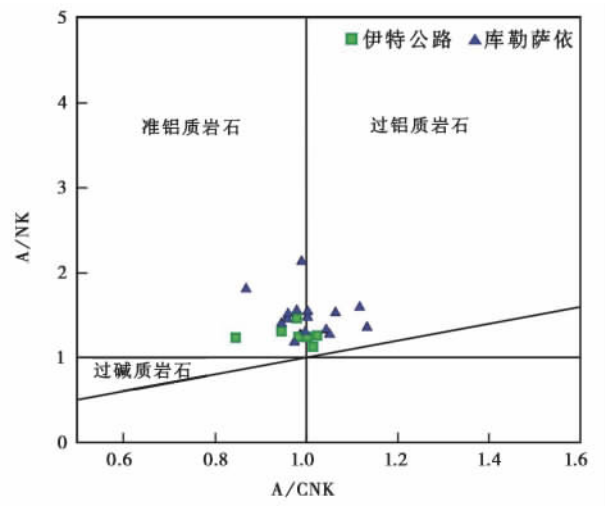


图 5 特克斯北中酸性火成岩 A/NK-A/CNK 图解

Fig. 5 The A/NK-A/CNK diagram of intermediate-acid igneous rocks from northern Tekesi area

两组火成岩的微量元素均表现出富集大离子亲石元素和亏损 Nb、Ta、Ti 等高场强元素的特征,与正常的岛弧带火成岩一致(图 7a)。库勒萨依岩体相对伊特公路沿线岩体的样品具有明显的 Sr 正异常和亏损 Y 的特征。除 XTT839 外,库勒萨依的样品 Sr 平均含量大于 400×10^{-6},范围在 $376.4\times10^{-6}\sim794\times10^{-6}$,Y 含量小于 19×10^{-6},Sr/Y 比值大于 20(28~96)。伊特公路沿线的样品 Sr 含量在 $206.6\times10^{-6}\sim576.4\times10^{-6}$,Y 含量大于 20×10^{-6}。在 Sr/Y-Y 图解中伊特公路样品均落入正常岛弧 ADR 范围内,而库勒萨依的样

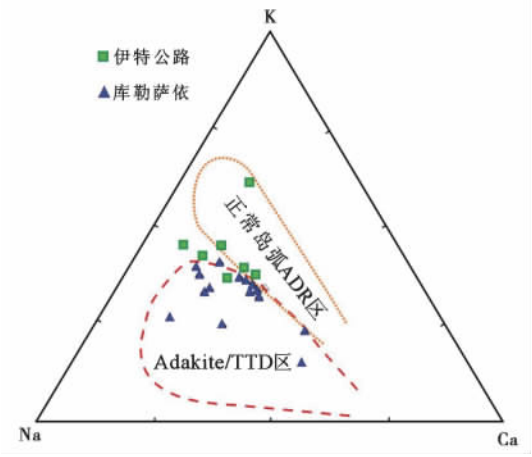


图 6 特克斯北中酸性火成岩的 Na-K-Ca 图解

Adakite /TTD 区和正常岛弧 ADR 区范围数据引自 Defant and Drummond(1993)和 Martin *et al*.(2005)

Fig. 6 Na-K-Ca diagram of intermediate-acid igneous rocks from northern Tekesi area

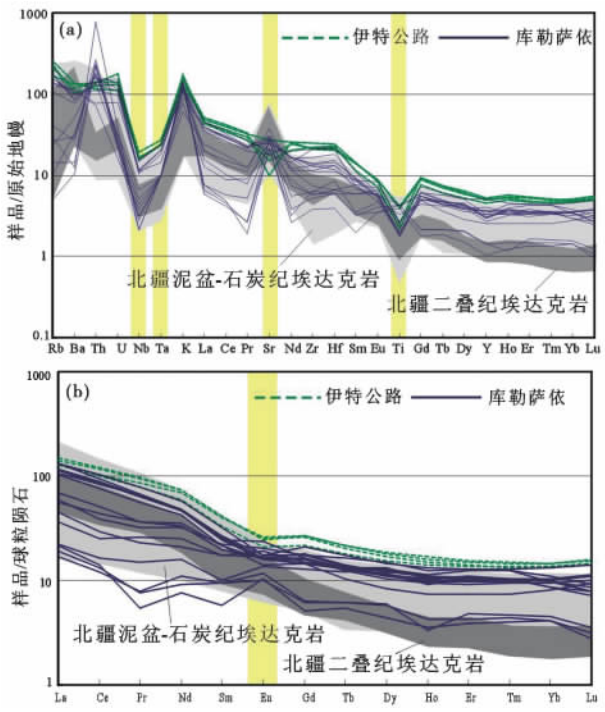


图 7 特克斯北中酸性火成岩微量元素蛛网图(a,原始地幔数据引自 Sun and McDonough,1989)与稀土元素配模式图(b,球粒陨石数据引自 Boynton,1984)

北疆泥盆-石炭纪埃达克岩数据范围来自:许继峰等,2001;李文明等,002;杨文平等,2005;熊小林等,2005;张连昌等,2006a,b;王强等,006;唐功建等,2009;Zhang HX,2005;北疆二叠纪埃达克岩数据范围引自:熊小林等,2001,2005;张连昌等,2006b;Zhao *et al*.,2008

Fig. 7 Primitive mantle-normalized trace element diagram(a, primitive mantle normalization values after Sun and McDonough, 989) and chondrite-normalized REE patterns(b, chondrite normalization values after Boynton, 1984) of intermediate-acid igneous rocks from northern Tekesi area

© 1994-2012 China Academic Journal Electronic Publishing House. All rights reserved. http://www.cnki.net

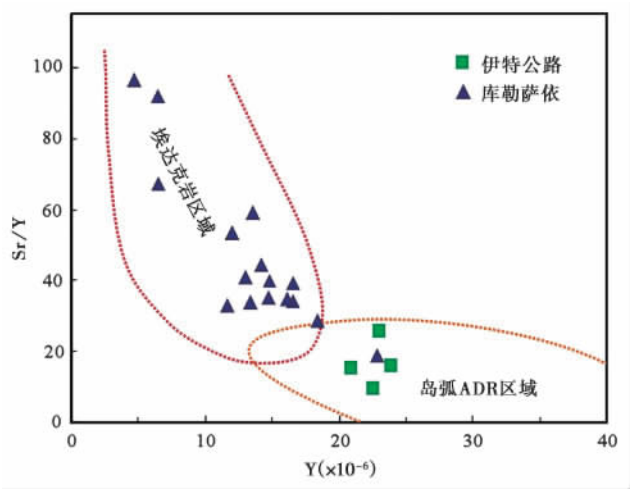


图 8 特克斯北中酸性火成岩的 Sr/Y-Y 图解(据 Defant and Drummond,1993)

Fig. 8 Sr/Y-Y diagram of intermediate-acid igneous rocks from northern Tekesi area(after Defant and Drummond,1993)

品主要落入埃达克岩区域(图 8),其中 XTT839 落于正常岛弧 ADR 区域,可能受到地壳物质的强烈混染。

两组样品的稀土元素配分曲线都显示右倾斜的特征,且伊特公路沿线的样品分布于上方(图 7b)。伊特公路沿线岩体的稀土元素总量达到 $147.3\times10^{-6}\sim178.6\times10^{-6}$,明显高于库勒萨依岩体(REE 总量平均值为 83.5×10^{-6})。另外伊特公路沿线的样品 Eu 具有明显的负异常($\delta Eu=0.73\sim0.79$),轻、重稀土都较富集;而库勒萨依样品 Eu 表现出弱负异常-正异常(δEu 集中在 0.8~1.19),亏损重稀土,Yb 含量小于 1.9×10^{-6},与埃达克岩的成分特征十分相似(Defant and Drummond,1990; Martin,1999)。

综上所述,特克斯北伊特公路沿线的石英钠长斑岩(大哈拉军山组)为典型的弧火成岩,而库勒萨依的石英闪长斑岩和花岗闪长斑岩具有与埃达克岩一致的地球化学特征,为典型的埃达克岩。

5 锶、钕同位素组成特征

Sr、Nd 同位素组成在中国科学院广州地球化学研究所同位素地球化学国家重点实验室完成,Nd 同位素组成由多收集器等离子体质谱(MC-ICP-MS)测定,分析流程等见梁细荣等(2002)。Sr 同位素组成由热电离质谱(TIMS)测定。伊特公路沿线岩体的 1 个样品和库勒萨依岩体的 4 个样品 Sr、Nd 同位素组成列出如表 3。

对 5 件火成岩样品进行了 Rb-Sr 和 Sm-Nd 同位素组成的分析,利用年龄 $t=342$Ma(伊特公路沿线的样品 $t=351$Ma)计算了 $(^{87}Sr/^{86}Sr)_i$、$(^{143}Nd/^{144}Nd)_i$ 和 $\varepsilon_{Nd}(t)$ 值(见表 3)。伊特公路沿线样品的 $(^{87}Sr/^{86}Sr)_i=0.704175$,$\varepsilon_{Nd}(t)$

表 3 特克斯北中酸性火成岩 Sr、Nd 同位素组成

Table 3 Sr and Nd composition of intermediate-acid igneous rocks from northern Tekesi area

位置	岩性	样品号	Rb ($\times10^{-6}$)	Sr ($\times10^{-6}$)	$^{87}Rb/^{86}Sr$	$^{87}Sr/^{86}Sr$	2SE	t (Ma)	$(^{87}Sr/^{86}Sr)_i$	Sm ($\times10^{-6}$)	Nd ($\times10^{-6}$)	$^{143}Nd/^{144}Nd$	$^{147}Sm/^{144}Nd$	2σ	$f_{Sm/Nd}$	$(^{143}Nd/^{144}Nd)_i$	$\varepsilon_{Nd}(t)$	t_{DM} (Ma)
伊特公路	钠长斑岩	XTT823	164.2	372	1.277427	0.710558	6	351	0.704175	6.136	32.72	0.512633	0.113381	8	-0.423585	0.512379	3.64	787.50
库勒萨依	石英闪长岩	XTT838	89.73	376.4	0.689730	0.707848	5	342	0.704490	3.314	19.65	0.512539	0.101967	9	-0.481614	0.512311	2.21	835.22
库勒萨依	花岗闪长岩	XTT840	113.1	593.5	0.551336	0.707460	7	342	0.704776	3.754	22.57	0.512562	0.100561	7	-0.488759	0.512337	2.72	793.96
库勒萨依	石英闪长岩	XTT842	82.15	649.9	0.365672	0.706426	7	342	0.704646	3.743	21.96	0.512658	0.103052	9	-0.476097	0.512427	4.48	679.76
库勒萨依	花岗闪长岩	XTT845	116.8	561.9	0.601408	0.707730	6	342	0.704802	4.013	22.69	0.512576	0.106931	8	-0.456377	0.512337	2.71	821.25

© 1994-2012 China Academic Journal Electronic Publishing House. All rights reserved. http://www.cnki.net

=3.64。库勒萨依4个样品的$(^{87}Sr/^{86}Sr)_i$、$(^{143}Nd/^{144}Nd)_i$和$\varepsilon_{Nd}(t)$变化范围都很小,$(^{87}Sr/^{86}Sr)_i$值较低,为0.7045~0.7048;$\varepsilon_{Nd}(t)$均为正值(+2.2~+4.5)。在$\varepsilon_{Nd}(t)$-$(^{87}Sr/^{86}Sr)_i$图解中,这些样品差异不明显,主要落在第一和第二象限分界线附近,沿着地幔趋势线排列(图9)。所有岩石样品均落于环太平洋新生代俯冲洋壳熔融形成的埃达克岩和天山泥盆-石炭纪埃达克岩区域内,与洋中脊玄武岩(MORB)Sr、Nd同位素组成比较接近,而与天山二叠纪新底侵铁镁质下地壳熔融成因的埃达克岩和天山元古代变质基底的Sr、Nd同位素组成明显不同。

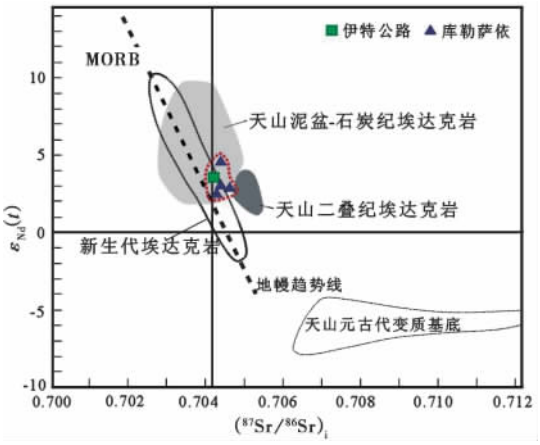


图9 特克斯北中酸性火成岩$\varepsilon_{Nd}(t)$-$(^{87}Sr/^{86}Sr)_i$图解(底图据赵振华等,2006)

Fig. 9 $\varepsilon_{Nd}(t)$-$(^{87}Sr/^{86}Sr)_i$ diagram of intermediate-acid igneous rocks from northern Tekesi area(after Zhao *et al.*,2006)

上述分析表明,伊特公路沿线和库勒萨依的源区岩石可能起源于亏损地幔。

6 讨论

6.1 岩石成因

一般来说,较老且冷的洋壳俯冲时,由于地热梯度较低,俯冲板片达到一定深度(通常是榴辉岩相)时先发生脱水作用,流体上升交代上覆地幔楔引发熔融并经历壳幔相互作用等,形成岛(陆)弧的钙碱性岩浆活动(Defant and Drummond,1993; Martin,1999)。现代俯冲带广泛分布的弧ADR系列岩石就形成于这样的岩浆活动过程。

如前文所述,伊特公路沿线的石英钠长斑岩具有富集大离子亲石元素(如Rb、Ba、Th、K),亏损高场强元素(Nd、Ta、Ti、Y等),稀土含量明显高,Sr、Nd同位素组成显示岩浆来源于亏损地幔等特征(表2、表3),符合典型的西天山大哈拉军山组岛弧火山岩的特征(Zhu *et al.*,2009; 李永军等,2010)。因此,伊特公路沿线的石英钠长斑岩的形成可能与西南天山古亚洲洋(南天山洋)俯冲过程有关。

库勒萨依岩体具有与埃达克岩一致地球化学特征:高Si、Na、Al和Sr,低Y和HREE以及高Sr/Y等(表2),在Sr/Y-Y图解中落于新生代埃达克岩区域(图8),其微量元素和稀土元素特征也与新生代埃达克岩一致,并且落于新疆北部泥盆-石炭纪埃达克岩分布范围,与伊特公路沿线岩体的元素组成完全不同(图7),因此可以用埃达克质岩石的成因模式来解释库勒萨依岩体的形成。

当前埃达克质岩石的成因模式主要包括:俯冲板片熔融(Defant and Drummond,1990,1993; Martin,1999; 许继峰等,2001; 熊小林等,2005; 王强等,2006; 李永军等,2008a);底侵玄武岩或加厚的下地壳镁铁质岩石熔融(熊小林等,2001; 张旗等,2001a,b; Wang *et al.*,2005; Zhao *et al.*,2008,2009);拆沉下地壳熔融(Xu *et al.*,2002; 王强等,2004)以及基性岩浆在地壳底部结晶分异和AFC作用(Feeley and Hacker,1995; Macpherson *et al.*,2006)等。

下地壳镁铁质岩石和拆沉下地壳物质熔融产生的埃达克岩通常比较富钾(Wang *et al.*,2005),具有负的$\varepsilon_{Nd}(t)$值和较高的$(^{87}Sr/^{86}Sr)_i$值(张旗等,2001a,b,2002)等特征。然而库勒萨依岩体相对富钠而贫钾,其Sr、Nd同位素组成也表明它们可能不是由底侵玄武质岩和加厚的下地壳熔融或拆沉下地壳熔融形成的。幔源岩浆在厚的地壳底部的分离结晶和混染作用使得石榴石析出造成岩浆中Y和HREE含量快速亏损(Feeley and Hacker,1995),对Sr含量几乎没有影响,这与库勒萨依岩体高Sr含量特征不符。此外,库勒萨依岩体正的$\varepsilon_{Nd}(t)$和较低的$(^{87}Sr/^{86}Sr)_i$值暗示了岩浆没有受到明显的陆壳物质混染作用。

库勒萨依岩体的Sr、Nd同位素组成与新生代环太平洋俯冲洋壳熔融形成的埃达克岩Sr、Nd同位素组成非常接近,在$\varepsilon_{Nd}(t)$-$(^{87}Sr/^{86}Sr)_i$图解中样品均落入新疆北部泥盆-石炭纪俯冲型埃达克岩范围,明显不同于天山元古代变质基底的成分(图9),表明它们可能是俯冲洋壳熔融的产物。其次,它们具有俯冲洋壳熔融成因埃达克岩的地球化学特征:富钠贫钾,与加厚下地壳熔融成因的富钾埃达克岩不同(Zhao *et al.*,2008)。此外,西天山在晚古生代处于岛弧环境,Wang *et al.*(2007)认为西天山在石炭纪存在年轻且热的洋壳俯冲事件。综上,库勒萨依岩体(埃达克岩)可能与早石炭世南天山洋俯冲熔融事件有关,属于新疆北部的"俯冲型"埃达克岩(赵振华等,2006)。

6.2 动力学过程及西天山地壳增生

新疆境内的天山造山带作为中亚造山带的重要组成部分,对其造山过程及陆壳生长的研究方兴未艾(肖文交等,2006; 高俊等,2009)。特别是晚古生代以来,伊犁-中天山板块南北缘的亚洲洋俯冲消减引发了大规模的岩浆活动,对这些火成岩的研究为揭示西天山造山过程与大陆增生提供了重要依据(朱永峰等,2005; 龙灵利等,2008; Wang *et al.*,2007; Zhu *et al.*,2009; 李永军等,2010)。本文通过对特克斯

© 1994-2012 China Academic Journal Electronic Publishing House. All rights reserved. http://www.cnki.net

北伊特公路沿线和库勒萨依火成岩的研究,可以重塑早石炭世南天山洋壳俯冲过程和西天山陆壳生长的历史。

根据前文中伊特公路沿线和库勒萨依两个岩体的年龄及岩石成因讨论,我们可以模拟出早石炭世南天山洋俯冲消减过程和西天山地壳增生方式的示意图(图10):

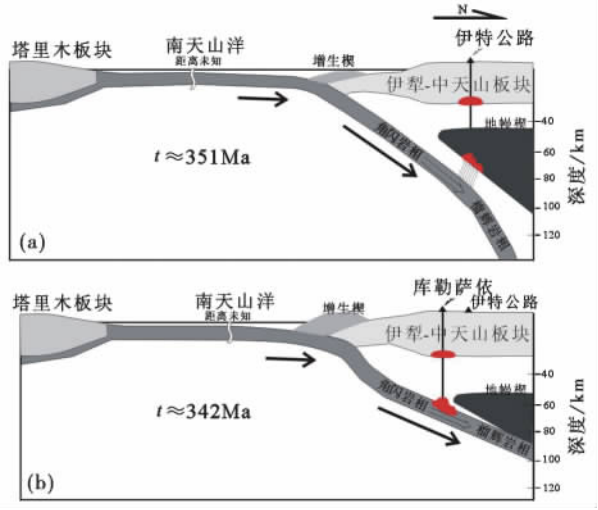


图10 南天山洋俯冲消减和成岩模式示意图(据 Xiao *et al.*, 2009 修改)

Fig. 10 The sketch map of subduction process of southern Tianshan ocean and genesis of intermediate-acid igneous rocks in northern Tekesi area(after Xiao *et al.*, 2009)

南天山洋可能早已开始俯冲(高俊等,2009),在早石炭世初期(~351Ma),较老且冷的洋壳在俯冲过程中达到一定的温压条件,发生脱水作用,流体上升并交代上覆地幔楔发生熔融,这与一般岛(陆)弧火成岩形成的模式类似(Defant and Drummond,1993)。通过发生流体交代、岩浆分离结晶和混合等复杂作用,最终岩浆上侵到伊特公路一带浅部地壳中形成石英钠长斑岩(图10a)。

在南天山洋的俯冲消减过程中,伊犁中天山板块南部形成增生楔,陆壳不断向南生长,洋脊位置也相对向北推近。随着俯冲作用的持续进行,在早石炭世中期(~342Ma),新生成的年轻且热的洋壳可能很接近俯冲带,并在较平缓倾角的俯冲过程中,由于摩擦作用和自身高热,板片在较浅的深度压力(角闪岩相向榴辉岩相转变)下即发生熔融,形成埃达克岩浆。岩浆上升过程中,部分熔体可能交代了地幔楔成分,使得岩浆中 $Mg^{\#}$ 升高。Xiong *et al.*(2005,2006,2009)通过实验岩石学研究将埃达克岩浆形成深度限制于石榴石(角闪石)和金红石稳定残留相,此压力对应地下深度约为50~80km。因此库勒萨依埃达克岩体的岩浆源区深度可能在50km以上(图10b)。

伊特公路沿线和库勒萨依的两组中酸性火成岩均形成于早石炭世南天山洋向北俯冲消减的岛(陆)弧环境,共同构成了岛(陆)弧带火成岩组合(典型的弧火成岩和埃达克岩)。对特克斯北中酸性火成岩的研究表明,早石炭世时南天山洋还未完全闭合。洋壳的持续俯冲使得亏损地幔成分加入新生地壳中,此时西天山地壳增生主要是侧向增生,增生物质主要为地幔楔成分、洋壳板片(即埃达克岩)和部分板片熔体交代地幔楔成分。

7 结论

(1)西天山特克斯北存在两组中酸性火成岩,伊特公路沿线的石英钠长斑岩为典型的弧火成岩,库勒萨依岩体为埃达克岩。两组火成岩均形成于南天山洋向北俯冲消减的岛(陆)弧环境,构成了岛(陆)弧带火成岩组合。

(2)早先俯冲的洋壳脱水交代地幔楔熔融以及壳幔相互作用,形成了伊特公路一带的中酸性火成岩。随着俯冲过程的持续,新生成的热洋壳可能直接发生熔融形成库勒萨依一带的埃达克岩。库勒萨依花岗闪长斑岩的 SIMS 锆石 U-Pb 年龄为 342.5±2.3Ma,表明早石炭世时南天山洋壳还在继续向伊犁板块之下俯冲,此时的西天山地壳增生以侧向增生为主,增生物质主要为流体交代的地幔楔成分、洋壳板片(埃达克岩)以及板片熔体交代的地幔楔成分。

致谢 审稿专家们对本文提出了宝贵的修改意见和建议,帮助作者提高了本文的论证,在此表示衷心感谢。

References

Boynton WV. 1984. Geochemistry of the rare earth elements: Meteorite studies. In: Henderson P (ed.). Rare Earth Element Geochemistry. Elservier, 63-114

Che ZC, Liu L, Liu HF and Luo JH. 1996. Review on the ancient Yili rift, Xingjiang, China. Acta Petrologica Sinica, 12(3): 478-489(in Chinese with English abstract)

Defant MJ and Drummond MS. 1990. Derivation of some modern arc magmas by melting of young subducted lithosphere. Nature, 347: 662-665

Defant MJ and Drummond MS. 1993. Mount St. Helens: Potential example of the partial melting of the subducted lithosphere in a volcanic arc. Geology, 21: 547-550

Feeley TC and Hacker MD. 1995. Intracrustal derivation of Na-rich andesitic and dacitic magmas: An example from Volcano Olague, Andean Central Volcanic Zone. Journal of Geology, 103: 213-225

Gao J, Li MS, Xiao XC, Tang YQ and He GQ. 1998. Paleozoic tectonic evolution of the Tianshan Orogen, northwestern China. Tectonophysics, 287: 213-231

Gao J, Long LL, Klemd R, Qian Q, Liu DY, Xiong XM, Su W, Liu W, Wang YT and Yang FQ. 2009. Tectonic evolution of the South Tianshan Orogen, NW China: Geochemical and age constraints of granitoid rocks. International Journal of Earth Sciences, 98: 1221-1238

Gao J, Qian Q, Long LL, Zhang X, Li JL and Su W. 2009. Accretionary orogenic process of Western Tianshan, China. Geological Bulletin of China, 28(12): 1804-1816(in Chinese with English abstract)

Gill JB. 1981. Orogenic Andesite and Plate Tectonics. Berlin: Springer, 1-390

Han BF, Guo ZJ, Zhang ZC, Zhang L, Chen JF and Song B. 2010. Age, geochemistry, and tectonic implications of a Late Paleozoic stitching

© 1994-2012 China Academic Journal Electronic Publishing House. All rights reserved. http://www.cnki.net

pluton in the North Tian Shan suture zone, western China. Geological Society of American Bulletin, 122: 627 – 640

Jahn BM. 2004. The Central Asian orogenic belt and growth of the continental crust in the Phanerozoic. Geological Society Special Publications, 226: 73 – 100

Li JY, Wang KZ, Li YP, Sun GH, Chu CH, Li LQ and Zhu ZX. 2006. Geomorphological features, crustal composition and geological evolution of the Tianshan Mountains. Geological Bulletin of China, 25(8): 895 – 909(in Chinese with English abstract)

Li XH, Liu Y, Li QL, Guo CH and Chamberlain KR. 2009. Precise determination of Phanerozoic zircon Pb/Pb age by multicollector SIMS without external standardization. Geochemistry Geophysics Geosystems, 10(4): Q04010, doi: 10.1029/2009GC002400

Li WM, Ren BC, Yang XK, Li YZ and Chen Q. 2002. The intermediate–acid intrusive magmatism and its geodynamic significance in Eastern Tianshan region. Northwestern Geology, 35(4): 41 – 64(in Chinese with English abstract)

Li YJ, Pang ZJ, Luan XD, Yang JQ, Wang XG, Zhang WF and Si GH. 2007. Disintegration of Tekesidaban granitic batholith and its significance for Mo prospecting, western Tianshan Mountains. Geotectonica et Metallogenia, 31(4): 435 – 440(in Chinese with English abstract)

Li YJ, Gu PY, Pang ZJ, Luan XD and Tong LP. 2008a. Identification of the adakite rocks of Kulesayi series and it's significance of Mo prospecting in the Tekesidaban of western Tianshan. Acta Petrologica Sinica, 24(12): 2713 – 2719(in Chinese with English abstract)

Li YJ, Zhang TJ. Luan XD, Wang XG, Yang GX and Tong LM. 2008b. Clarification of Late Paleozoic unconformities in the Tekes Daban area of West Tianshan and its geological significance. Acta Geoscientica Sinica, 29(2): 145 – 153(in Chinese with English abstract)

Li YJ, Hu KL, Zhou JB, Tong LL and Tong LM. 2010. Early Carboniferous volcano–magmatism and related mineralization in Yishijilike Mountain, Western Tianshan. Earth Science, 35(2): 235 – 244(in Chinese with English abstract)

Li ZC, Li YJ, Li JH, Luan XD and Guo WJ. 2006. Geochemical characteristics of the Dahalajunshan Formation volcanic rocks and their implications on the tectonic setting in Awulale area. Xinjiang Geology, 24(2): 120 – 124(in Chinese with English abstract)

Liang XR, Wei GJ, Li XH and Liu Y. 2002. Rapid and precise measurement for $^{143}Nd/^{144}Nd$ isotopic ratios using a multi-collector inductively coupled plasma mass spectrometer. Rock and Mineral Analysis, 21(4): 247 – 251(in Chinese with English abstract)

Liu Y, Liu HC and Li XH. 1996. Simultaneous and precise determination of 40 trace element in rock samples using ICP–MS. Geochimica, 25(6): 552 – 558(in Chinese with English abstract)

Long LL, Gao J, Qian Q, Xiong XM, Wang JB, Wang YW and Gao LM. 2008. Geochemical characteristics and tectonic settings of Carboniferous volcanic rocks from Yili region, western Tianshan. Acta Petrologica Sinica, 24(4): 699 – 710(in Chinese with English abstract)

Ludwig KR. 2003. User's manual for Isoplot 3.00: A geochronological toolkit for Microsoft Excel. Berkeley Geochronology Centre Special Publication, No. 4: 1 – 70

Macpherson CG, Dreher ST and Thirlwall MF. 2006. Adakites without slab melting: High pressure differentiation of island arc magma, Mindanao, the Philippines. EPSL, 243: 581 – 593

Martin H. 1999. Adakitic magmas: Modern analogues of Archaean granitoids. Lithos, 46: 411 – 429

Martin H, Smithies RH, Rapp R, Moyen JF and Champion D. 2005. An overview of adakite, tonolite–trondhjemite–granodiorite (TTG), and sanukitoid: Relationships and some implications for crustal evolution. Lithos, 79: 1 – 24

Sun SS and McDonough WF. 1989. Chemical and isotopic systematics of oceanic basalts: Implications for mantle composition and processes. In: Saunders AD and Norry MJ (eds.). Magmatism in the Ocean Basins. Geological Society London Special Publications, 42: 313 – 345

Tang GJ, Wang Q, Zhao ZH, Wyman DA, Chen HH, Jia XH and Jiang ZQ. 2009. Geochronology and geochemistry of the ore–bearing porphyries in the Baogutu area (western Junggar): Petrogenesis and their implications for tectonics and Cu–Au mineralization. Earth Science, 34(1): 56 – 74(in Chinese with English abstract)

Tang GJ, Wang Q, Wyman DA, Sun M, Li ZX, Zhao ZH, Sun WD, Jia XH and Jiang ZQ. 2010. Geochronology and geochemistry of Late Paleozoic magmatic rocks in the Lamasu–Dabate area, northwestern Tianshan(West China): Evidence for a tectonic transition from arc to post-collisional setting. Lithos, 119: 293 – 411

Wang B, Cluzel D, Shu LS, Faure M, Charvet J, Chen Y, Meffre S and de Jong K. 2009. Evolution of calc-alkaline to alkaline magmatism through Carboniferous convergence to Permian transcurrent tectonics, western Chinese Tianshan. International Journal of Earth Sciences, 98: 1275 – 1298

Wang JB and Xu X. 2006. Post-collisional tectonic evolution and metallogenesis in northern Xinjiang. China. Acta Geologica Sinica, 80(1): 23 – 31(in Chinese with English abstract)

Wang Q, Zhao ZH, Bai ZH, Bao ZW, Xiong XL, Mei HJ, Xu JF and Wang YX. 2003. Carboniferous adakites and Nb–enriched arc basaltic rocks association in the Alataw Mountains, north Xinjiang: Interactions between slab melt and mantle peridotite and implications for crustal growth. Chinese Science Bulletin, 48(19): 2108 – 2115

Wang Q, Zhao ZH, Xu JF, Bai ZH, Wang JX and Liu CX. 2004. The geochemical comparison between the Tongshankou and Yinzu adakitic intrusive rocks in southeastern Hubei: (delaminated) lower crustal melting and the genesis of porphyry copper deposit. Acta Petrologica Sinica, 20(2): 351 – 360(in Chinese with English abstract)

Wang Q, McDermontt F, Xu JF, Bellon H and Zhu YT. 2005. Cenozoic K–rich adakitic volcanic rocks in the Hohxil area, northern Tibet: Lower-crustal melting in an intracontinental setting. Geology, 33: 465 – 468

Wang Q, Zhao ZH, Xu JF, Wyman DA, Xiong XL, Zi F and Bai ZH. 2006. Carboniferous adakite–high–Mg andesite–Nb–enriched basaltic rock suites in the Northern Tianshan area: Implications for Phanerozoic crustal growth in the Central Asia Orogenic Belt and Cu–Au mineralization. Acta Petrologica Sinica, 22(1): 11 – 30(in Chinese with English abstract)

Wang Q, Wyman DA, Zhao ZH, Xu JF, Bai ZH, Xiong XL, Dai TM, Li CF, Chu ZY. 2007. Petrogenesis of Carboniferous adakites and Nb–enriched arc basalts in the Alataw area, northern Tianshan Range (western China): Implications for Phanerozoic crustal growth in the Central Asia orogenic belt. Chemical Geology, 236: 42 – 64

Whitehouse MJ, Claesson S, Sunde T and Vestin J. 1997. Ion–microprobe U–Pb zircon geochronology and correlation of Archaean gneisses from the Lewisian Complex of Gruinard Bay, Northwest Scotland. Geochim. Cosmochim. Acta, 61: 4429 – 4438

Wiedenbeck M, Alle P, Corfu F, Griffin WL, Meier M, Oberli F, Quadt AV, Roddick JC and Spiegel W. 1995. Three natural zircon standards for U–Th–Pb, Lu–Hf, trace-element and REE analyses. Geostandards Newsletter, 19: 1 – 23

Windley BF, Alexeiev D, Xiao WJ, Kroner A and Badarch G. 2007. Tectonic models for accretion of the Central Asian Orogenic Belt. Journal of the Geological Society, London, 164: 31 – 47

Xia LQ, Xu XY, Xia ZC, Li XM, Ma ZP and Wang LS. 2004. Petrogenisis of Carboniferous rift-related volcanic rocks in the Tianshan, northwestern China. Geological Society of America Bulletin, 116: 419 – 433

Xia LQ, Xia ZC, Xu XY, Li XM and Ma ZP. 2008. Petrogenisis of Carboniferous–Early Permian rift-related volcanic rocks in the Tianshan and its neighboring area, northwestern China. Northwestern Geology, 41(4): 1 – 68(in Chinese with English abstract)

Xiao WJ, Windley BF, Badarch G, Sun S, Li J, Qin K and Wang Z. 2004. Palaeozoic accretionary and convergent tectonics of the southern Altaids: Implications for the lateral growth of Central Asia. Journal of the Geological Society, London, 161: 339 – 342

Xiao WJ, Han CM, Yuan C, Chen HL, Sun M, Lin SF, Li ZL, Mao QG,

© 1994-2012 China Academic Journal Electronic Publishing House. All rights reserved. http://www.cnki.net

Zhang JE, Sun S and Li JL. 2006. Unique Carboniferous-Permian tectonic-metallogenic framework of Northern Xinjiang(NW China): Constraints for the tectonics of the southern Paleoasian Domain. Acta Petrologica Sinica, 22(5): 1062 – 1076(in Chinese with English abstract)

Xiao WJ, Windley BF, Huang BC, Han CM, Yuan C, Chen HL, Sun M, Sun S and Li JL. 2009. End-Permian to Mid-Triassic termination of the accretionary processes of the southern Altaids: Implications for the geodynamic evolution, Phanerozoic continental growth, and metallogeny of Central Asia. International Journal of Earth Sciences, 98: 1189 – 1217

Xiao WJ, Huang BC, Han CM, Sun S and Li JL. 2010. A review of the western part of the Altaids: A key to understanding the architecture of accretionary orogens. Gondwana Research, 18: 253 – 273

Xiong XL, Zhao ZH, Bai ZH, Mei HJ, Xu JF and Wang Q. 2001. Origin of Awulale adakitic sodium-rich rocks in western Tianshan: Constraints for Nd and Sr isotopic compositions. Acta Petrologica Sinica, 17(4): 514 – 522(in Chinese with English abstract)

Xiong XL, Adam J and Green TH. 2005. Rutile stability and rutile/melt HFSE partitioning during partial melting of hydrous basalt: Implications for TTG genesis. Chemical Geology, 218: 339 – 359

Xiong XL, Cai ZY, Niu HC, Chen YB, Wang Q, Zhao ZH and Wu JH. 2005. The Late Paleozoic adakites in eastern Tianshan area and their metallogenetic significance. Acta Pstrologica Sinica, 21(3): 967 – 976(in Chinese with English abstract)

Xiong XL, Adam J and Green TH. 2006. Trace element characteristics of partial melts of metabasalt and the formation conditions of adakitic melts. Science in China, (Series D), 49(9): 915 – 925

Xiong XL, Keppler H, Audétat A, Gudfinnsson G, Sun WD, Song MS, Xiao WS and Li Y. 2009. Experimental constraints on rutile saturation during partial melting of metabasalt at the amphibolite to eclogite transition, with applications to TTG genesis. American Mineralogist, 94: 1175 – 1186

Xu JF, Mei HJ, Yu XY, Bai ZH, Niu HC, Chen FR, Zhen ZP and Wang Q. 2001. Adakites related to subduction in the northern margin of Junggar arc for the Late Paleozoic: Products of slab melting. Chinese Science Bulletin, 46(15): 1313 – 1317

Xu JF, Shinjo R, Defant MJ, Wang Q and Rapp RP. 2002. Origin of Mesozoic adakitic intrusive rock in the Ningzhen area of East China: Partial melting of delaminated lower continental crust? Geology, 30(12): 1111 – 1114

Xue YX and Zhu YF. 2009. Zircon SHRIMP chronology and geochemistry of Haladala gabbro in southwestern Tianshan Mts. Acta Petrologica Sinica, 25(6): 1353 – 1363(in Chinese with English abstract)

Yang WP, Zhang ZC, Zhou G, Yan SH, He LX and Chen BL. 2005. Discovery of the Xileketehalsu porphyry copper deposit on the southern margin of the Altay copper metallogenic belt. Geology in China, 32(1): 107 – 114(in Chinese with English abstract)

Zhang HX, Niu HC, Sato H, Yu XY, Shan Q, Zhang BY, Ito J and Nagao T. 2005. Late Paleozoic adakites and Nb-enriched basalts from northern Xinjiang, Northwest China: Evidence for the southward subduction of the Paleo-Asian Oceanic Plate. The Island Arc, 14: 55 – 68

Zhang LC, Wan B, Jiao XJ and Zhang R. 2006a. Characteristics and geological significance of adakitic rocks in copper-bearing porphyry in Baogutu, western Junggar. Geology in China, 33(3): 626 – 631(in Chinese with English abstract)

Zhang LC, Wang B, Li WQ and Tang HF. 2006b. Geochemistry and tectonic setting of copper-bearing porphyries on the southern margin of Tuha basin, Xinjiang. Acta Petrologica Sinica, 22(1): 225 – 235(in Chinese with English abstract)

Zhang Q, Wang YL and Wang Y. 2001a. Preliminary study on the components of the lower crust in East China Plateau during Yanshanian Period: Constraints on Sr and Nd isotopic compositions of adakite-like rocks. Acta Petrologica Sinica, 17(4): 505 – 513(in Chinese with English abstract)

Zhang Q, Wang Y, Qian Q, Yang JH, Wang YL, Zhao TP and Guo GJ. 2001b. The characteristics and tectonic-metallogenic significance of the adakites in Yanshan Period from eastern China. Acta Petrologica Sinica, 17(2): 236 – 244(in Chinese with English abstract)

Zhang Q, Wang Y, Liu W and Wang YL. 2002. Adakite: Its characteristics and implications. Geological Bulletin of China, 21(7): 431 – 435(in Chinese with English abstract)

Zhao ZH, Wang Q, Xiong XL, Zhang HX, Niu HC, Xu JF, Bai ZH and Qiao YL. 2006. Two types of adakites in North Xinjiang, China. Acta Petrologica Sinica, 22(5): 1249 – 1265(in Chinese with English abstract)

Zhao ZH, Xiong XL, Wang Q, Wyman DA, Bao ZW and Qiao YL. 2008. Underplating-related adakites in Xinjiang Tianshan, China. Lithos, 102: 374 – 391

Zhao ZH, Xiong XL, Wang Q, Bai ZH and Qiao YL. 2009. Late Paleozoic underplating in North Xinjiang: Evidence from shoshonites and adakites. Gondwana Research, 16: 216 – 226

Zhu MT, Wu G, Xie HJ, Liu J and Zhang LC. 2011. Geochronology and geochemistry of the Kekesai intrusion in western Tianshan, NW China and its geological implications. Acta Petrologica Sinica, 27(10): 3041 – 3054(in Chinese with English abstract)

Zhu YF, Zhang LF, Gu LB, Guo X and Zhou J. 2005. The zircon SHRIMP chronology and trace element geochemistry of the Carboniferous volcanic rocks in western Tianshan Mountains. Chinese Science Bulletin, 50: 2201 – 2212

Zhu YF, Zhou J and Guo X. 2006a. Petrology and Sr-Nd isotopic geochemistry of the carboniferous volcanic rocks in the western Tianshan Mountains, NW China. Acta Petrologica Sinica, 22(5): 1341 – 1350(in Chinese with English abstract)

Zhu YF, Zhou J, Song B, Zhang LF and Guo X. 2006b. Age of the "Dahalajunshan" Formation in Xinjiang and its disintegration. Geology in China, 33(3): 487 – 497(in Chinese with English abstract)

Zhu YF, Guo X, Song B, Zhang LF and Gu LB. 2009. Petrology, Sr-Nd-Hf isotopic geochemistry and zircon chronology of the Late Palaeozoic volcanic rocks in the southwestern Tianshan Mountains, Xinjiang, NW China. Journal of the Geological Society, London, 166: 1085 – 1099

Zhu YF, An F, Xue YX, Chen B and Zhang LF. 2010. Zircon U-Pb age for Kesang Rondong volcanic rocks, Southwet Tianshan Mts., Tekes, Xinjiang. Acta Petrologica Sinica, 26(8): 2255 – 2263(in Chinese with English abstract)

Zhu ZM, Zhao ZH, Xiong XL and Han JW. 2010. Petrogeochemistry of Late Paleozoic gabbroic rocks from Tekes County in West Tianshan Mountains. Acta Petrologica et Mineralogica, 29(6): 675 – 690(in Chinese with English abstract)

Zhu ZX, Li JY, Dong LH, Wang KZ, Zhang XF and Xu SQ. 2011. Geological characteristics and tectonic significance of Palezoic intrusive rocks in Western Tianshan of Xinjiang Province. Earth Science Frontiers, 18(2): 170 – 179(in Chinese with English abstract)

附中文参考文献

车自成, 刘良, 刘洪福, 罗金海. 1996. **论伊犁古裂谷. 岩石学报**, 12(3): 478 – 489

高俊, 钱青, 龙灵利, 张喜, 李继磊, 苏文. 2009. **西天山的增生造山过程. 地质通报**, 28(12): 1804 – 1816

李锦轶, 王克卓, 李亚萍, 孙桂华, 楮春华, 李丽群, 朱志新. 2006. **天山山脉地貌特征、地壳组成与地质演化. 地质通报**, 25(8): 895 – 909

李文明, 任秉琛, 杨兴科, 李有柱, 陈强. 2002. **东天山中酸性侵入岩浆作用及其地球动力学意义. 西北地质**, 35(4): 41 – 64

李永军, 庞振甲, 栾新东, 杨俊泉, 王小刚, 张文峰, 司国辉. 2007. **西天山特克斯达坂花岗岩基的解体及钼找矿意义. 大地构造与成矿学**, 31(4): 435 – 440

李永军, 辜平阳, 庞振甲, 栾新东, 佟丽萍. 2008a. **西天山特克斯达坂**

© 1994-2012 China Academic Journal Electronic Publishing House. All rights reserved. http://www.cnki.net

库勒萨依序列埃达克岩的确立及钼找矿意义. 岩石学报,24(12): 2713 – 2719

李永军,张天继,栾新东,王小刚,杨高学,佟黎明. 2008b. 西天山特克斯达坂晚古生代若干不整合的厘定及地质意义. 地球学报,29(2): 145 – 153

李永军,胡克亮,周继兵,佟丽莉,佟黎明. 2010. 西天山伊什基里克山早石炭世火山岩浆作用及其成矿. 地球科学,35(2): 235 – 244

李注苍,李永军,李景宏,栾兴东,郭文杰. 2006. 西天山阿吾拉勒一带大哈拉军山组火山岩地球化学特征及构造环境分析. 新疆地质,24(2): 120 – 124

梁细荣,韦刚健,李献华,刘颖. 2002. 多收集器等离子体质谱快速精确测定钕同位素比值. 岩矿测试,21(4): 247 – 251

刘颖,刘海臣,李献华. 1996. 用 ICP-MS 准确测定岩石样品中的 40 余种微量元素. 地球化学,25(6): 552 – 558

龙灵利,高俊,钱青,熊贤明,王京彬,王玉往,高立明. 2008. 西天山伊犁地区石炭纪火山岩地球化学特征及构造环境. 岩石学报,24(4): 699 – 710

唐功建,王强,赵振华,Wyman DA,陈海红,贾小辉,姜子琦. 2009. 西准噶尔包古图成矿斑岩年代学与地球化学: 岩石成因与构造、铜金成矿意义. 地球科学,34(1): 56 – 74

王京彬,徐新. 2006. 新疆北部后碰撞构造演化与成矿. 地质学报,80(1): 23 – 31

王强,赵振华,白正华,熊小林,梅厚钧,许继峰,包志伟,王一先. 2003. 新疆阿拉套山石炭纪埃达克岩、富 Nb 岛弧玄武岩: 板片熔体与地幔橄榄岩相互作用及地壳增生. 科学通报 48(12): 1342 – 1349

王强,赵振华,许继峰,白正华,王建新,刘成新. 2004. 鄂东南铜山口、殷祖埃达克质(adakitic)侵入岩的地球化学特征对比:(拆沉)下地壳熔融与斑岩铜矿的成因. 岩石学报,20(2): 351 – 360

王强,赵振华,许继峰,Wyman DA,熊小林,资峰,白正华. 2006. 天山北部石炭纪埃达克岩-高镁安山岩-富 Nb 岛弧玄武质岩: 对中亚造山带显生宙地壳增生与铜金成矿的意义. 岩石学报,22(1): 11 – 30

夏林圻,夏祖春,徐学义,李向民,马中平. 2008. 天山及邻区石炭纪–早二叠世裂谷火山岩岩石成因. 西北地质,41(4): 1 – 68

肖文交,韩春明,袁超,陈汉林,孙敏,林寿发,厉子龙,毛启贵,张继恩,孙枢,李继亮. 2006. 新疆北部石炭纪-二叠纪独特的构造-成矿作用: 对古亚洲洋构造域南部大地构造演化的制约. 岩石学报,22(5): 1062 – 1076

熊小林,赵振华,白正华,梅厚钧,许继峰,王强. 2001. 西天山阿吾拉勒埃达克质岩石成因: Nd 和 Sr 同位素组成的限制. 岩石学报,17(4): 514 – 522

熊小林,蔡志勇,牛贺才,陈义兵,王强,赵振华,吴金花. 2005. 东天山晚古生代埃达克岩成因及铜金成矿意义. 岩石学报,21(3): 967 – 976

许继峰,梅厚钧,于学元,白正华,牛贺才,陈繁荣,郑作平,王强. 2001. 准噶尔北缘晚古生代岛弧中与俯冲作用有关的 adakite 火山岩: 消减板片部分熔融的产物. 科学通报,46(8): 684 – 687

薛云兴,朱永峰. 2009. 西南天山哈拉达拉岩体的锆石 SHRIMP 年代学及地球化学研究. 岩石学报,25(6): 1353 – 1363

杨文平,张招崇,周刚,闫升好,何立新,陈柏林. 2005. 阿尔泰铜矿带南缘希勒克特哈腊苏斑岩铜矿的发现及其意义. 中国地质,32(1): 107 – 114

张连昌,万博,焦学军,张锐. 2006a. 西准包古图含铜斑岩的埃达克岩特征及其地质意义. 中国地质,33(3): 626 – 631

张连昌,万博,李文铅,唐红峰. 2006b. 新疆吐哈盆地南缘铜矿带含矿斑岩的地球化学及形成环境. 岩石学报,22(1): 225 – 235

张旗,王元龙,王焰. 2001a. 燕山期中国东部高原下地壳组成初探: 埃达克质岩 Sr、Nd 同位素制约. 岩石学报,17(4): 505 – 513

张旗,王焰,钱青,杨进辉,王元龙,赵太平,郭光军. 2001b. 中国东部燕山期埃达克岩的特征及其构造-成矿意义. 岩石学报,17(2): 236 – 244

张旗,王焰,刘伟,王元龙. 2002. 埃达克岩的特征及其意义. 地质通报,21(7): 431 – 435

赵振华,王强,熊小林,张海祥,牛贺才,许继峰,白正华,乔玉楼. 2006. 新疆北部的两类埃达克岩. 岩石学报,22(5): 1249 – 1265

朱明田,武广,解洪晶,刘军,张连昌. 2011. 新疆西天山科克赛岩体年代学、地球化学及地质意义. 岩石学报,27(10): 3041 – 3054

朱永峰,张立飞,古丽冰,郭璇,周晶. 2005. 西天山石炭纪火山岩 SHRIMP 年代学及其微量元素地球化学研究. 科学通报,50(18): 2004 – 2014

朱永峰,周晶,郭璇. 2006a. 西天山石炭纪火山岩岩石学及 Sr-Nd 同位素地球化学研究. 岩石学报,22(5): 1341 – 1350

朱永峰,周晶,宋彪,张立飞,郭璇. 2006b. 新疆“大哈拉军山组”火山岩的形成时代问题及其解体方案. 中国地质,33(3): 487 – 497

朱永峰,安芳,薛云兴,陈博,张立飞. 2010. 西南天山特克斯科桑溶洞火山岩的锆石 U-Pb 年代学研究,岩石学报,26(8): 2255 – 2263

朱志敏,赵振华,熊小林,韩江伟. 2010. 西天山特克斯晚古生代辉长岩岩石地球化学. 岩石矿物学杂志,29(6): 675 – 690

朱志新,李锦轶,董连慧,王克卓,张晓帆,徐仕琪. 2011. 新疆西天山古生代侵入岩的地质特征及构造意义. 地学前缘,18(2): 170 – 179

© 1994-2012 China Academic Journal Electronic Publishing House. All rights reserved. http://www.cnki.net